JBC Papers in Press. Published on November 14, 2011 as Manuscript M111.262543
The latest version is at http://www.jbc.org/cgi/doi/10.1074/jbc.M111.262543

UP-REGULATION OF THE NEURONAL NICOTINIC RECEPTOR α7 BY HIV-GP120: POTENTIAL IMPLICATIONS FOR HIV ASSOCIATED NEUROCOGNITIVE DISORDER

Leomar Y. Ballester[1], Coral M. Capó-Vélez[1], Wilfredo F. García-Beltrán[1], Félix M. Ramos[1], Edwin Vázquez-Rosa[1], Raymond Ríos, José R. Mercado[1], Roberto I. Meléndez[2], José A. Lasalde-Dominicci[1]

[1]University of Puerto Rico, Río Piedras Campus
Department of Biology, PO Box 23360, San Juan, P.R. 00931-3360
[2]University of Puerto Rico, Medical Sciences Campus
Department of Anatomy and Neurobiology, PO Box 365067, San Juan P.R. 00936-5067
Address correspondence to: José A. Lasalde-Dominicci, PhD, PO Box 23360
San Juan, Puerto Rico 00931-3360, Email:jlasalde@gmail.com

About 30-50% of the over 30 million HIV-infected subjects develop neurological complications ranging from mild symptoms to dementia. HIV does not infect neurons, and the molecular mechanisms behind HIV-associated neurocognitive decline are not understood. There are several hypotheses to explain the development of dementia in HIV+ individuals, including neuroinflammation mediated by infected microglia and neuronal toxicity by HIV proteins. A key protein associated with the neurological complications of HIV, gp120, forms part of the viral envelope and can be found in the CSF of infected individuals. HIV-1-gp120 interacts with several receptors including CD4, CCR5, CXCR4, and nicotinic acetylcholine receptors (nAChRs). However, the role of nAChRs in HIV-associated neurocognitive disorder (HAND) has not been investigated. We studied the effects of $gp120_{IIIB}$ on the expression and function of the nicotinic receptor α7 (α7-nAChR). Our results show that gp120, through activation of the CXCR4 chemokine receptor, induces a functional up-regulation of α7-nAChRs. Since α7-nAChRs have a high permeability to Ca^{2+}, we performed TUNEL staining to investigate the effects of receptor up-regulation on cell viability. Our data revealed an increase in cell death, which was blocked by the selective antagonist α-bungarotoxin. The *in-vitro* data is supported by RT-PCR and Western blot analysis confirming a remarkable up-regulation of the α7-nAChR in gp120-transgenic mice brains. Specifically, α7-nAChR up-regulation is observed in mouse striatum, a region severely affected in HIV+ patients. In summary, CXCR4 activation induces up-regulation of α7-nAChR, causing cell death, suggesting that α7-nAChR is a previously unrecognized contributor to the neurotoxicity associated with HIV infection.

Introduction

Over 30 million people are infected with HIV worldwide (*1*). In addition to the health problems caused by immunosuppression, HIV infection causes HIV-associated neurocognitive disorder (HAND), a neurodegenerative disease that leads to severe cognitive, motor, and behavioral disturbances. Before the introduction of highly active antiretroviral therapy (HAART), 30%-50% of HIV-infected patients developed HAND; after the incorporation of HAART as part of HIV treatment, the incidence decreased to approximately 10% (*2-5*). Nevertheless, in association with the existence of HAART treatment, which prolongs the life of HIV-infected individuals, there has been an increase to approximately 30% in the number of individuals who develop a milder form of neurocognitive dysfunction known as minor cognitive-motor disorder (MCMD), which is characterized by neurological deficits that do not interfere with every day functioning (*6*). Therefore, despite the reduction in HAND incidence, its prevalence is expected to increase due the improved care of HIV-infected patients. When evaluating the alterations in the incidence of HAND as a result of HAART, it is important to consider that of the approximately 30 million HIV-infected individuals worldwide, only 2 million have access to HAART (*1*). In addition, HIV infection continues to be the most common cause of dementia in young adults in the United States (*7, 8*). This suggests that HAND will continue to be an important health care problem in the United States and worldwide.

The presence of neurological symptoms in HIV-infected patients is an interesting finding, considering that HIV does not infect neurons directly. The molecular mechanisms by which HIV infection leads to neurocognitive decline are not fully understood, but several hypotheses have emerged to explain the development of neurocognitive impairment in HIV+ individuals. Two potential mechanisms by which HIV

infection could interfere with normal brain functioning are 1) chemokine-induced neuroinflammation mediated by infected macrophages/microglia and 2) direct neuronal toxicity induced by soluble HIV proteins (*9*). HIV-1-gp120, a glycoprotein that forms part of the envelope of HIV-1 particles, can be found in the cerebrospinal fluid of HIV+ individuals, and it has been shown to have neurotoxic effects in cell cultures (*9-13*). HIV-1-gp120 interacts with several receptors found in the central nervous system (CNS), including CD4, CCR5, and CXCR4, as well as nicotinic acetylcholine receptors (nAChRs) (*14-16*). Several lines of evidence suggest the potential involvement of the nicotinic acetylcholine receptor α7-nAChR in HIV neuropathology (*17-19*); however, the role that nAChRs may play in the development of HAND has not been investigated.

In order for HIV-1 to infect cells, it must bind the CD4 receptor and either the CCR5 or CXCR4 co-receptor. Interestingly, during the course of infection, HIV-1 evolves from an M-tropic (CCR5-dependent) variant that primarily infects macrophages to a T-tropic (CXCR4-dependent) variant that primarily infects T cells (*15, 20*). The increase in HIV particles with tropism for CXCR4 receptor correlates with the development of HAND (*20, 21*). Studies have shown that gp120 not only binds to CXCR4, but also activates its signaling pathway (*22*). CXCR4 activation by Stromal cell-derived growth factor (SDF-1α), the endogenous agonist of CXCR4, has been shown to rapidly up-regulate the early growth response gene 1 (Egr1), a transcription factor known to drive the expression of the α7-nAChR (*23, 24*). Furthermore, it has been shown that SDF-1α is secreted by astrocytes during inflammation and is increased in response to macrophage activation by HIV infection (*25*). Consequently, we designed experiments to study the effects of gp120 on the expression and function of α7-nAChRs in SH-SY5Y neuroblastoma cells, which endogenously express α7-nAChRs and CXCR4 receptors (*26*). Our results show that CXCR4 activation, by gp120 or SDF-1α, leads to an increase in α7-nAChR activity that can culminate in cell death. In addition, Western Blot and qRT-PCR analysis confirm up-regulation of α7-nAChR in transgenic mice expressing the HIV-gp120 gene.

Methods

Fluorescent α-bungarotoxin (bgtx) binding: SH-SY5Y cells were grown in four-well tissue culture slides (Nalge Nunc International, Rochester, NY). Cell culture media was removed, the cells were washed with phosphate buffered saline (PBS), fixed by incubation with 4% paraformaldehyde for 10 minutes followed by incubation with 1% bovine serum albumin (BSA) for 10 minutes. The cells were washed with PBS and then incubated with Alexa Fluor 488-conjugated α-bungarotoxin (Invitrogen Corporation, Carlsbad, CA) 1:50 for 1 hour at room temperature. Cells were then washed 3 times with PBS, cover slips mounted with 90% glycerol and analyzed with an Axiovert 200M confocal microscope.

Electrophysiology: Whole-cell currents were measured in the whole-cell configuration of the patch clamp technique using an Axopatch 200B amplifier (Axon Instruments, Inc., Foster City, CA). The bath solution contained (in mM) 140 NaCl, 4 KCl, 2 $CaCl_2$, 1 $MgCl_2$, 5 HEPES, 10 glucose, pH 7.4, ~280 mosmol/kg. The pipette solution contained (in mM) 145 KCl, 6 $MgCl_2$, 7.2 K_2HPO_4, 2.8 KH_2PO_4, 5 EDTA, pH 7.4, ~270 mosmol/kg. Pipettes were pulled from thick-wall borosilicate glass (World Precision Instruments, Inc., Sarasota, FL) with a multistage P-87 Flaming-Brown micropipette puller (Sutter Instruments Co., San Rafael, CA) and fire-polished. Pipette resistance was 2-4 MΩ, and a 1%-2% agar bridge with composition similar to the bath solution was utilized as the reference electrode. Chemicals were purchased from Sigma Chemicals (St. Louis, MO). Whole-cell current traces were filtered at 2 kHz and acquired at 10 kHz. Currents were measured in response to a 1-second pulse of 500 mM acetylcholine at a holding potential of -100 mV. Pulse generation, data collection, and analyses were carried out with Clampex 10.1 (Molecular Devices, Inc., Sunnyvale, CA).

Calcium flux assay: SH-SY5Y cells were grown on cover slips and treated with 0.15 nM gp120 overnight followed by incubation on non-supplement media with 10μM Fluo4-AM for 30 minutes in the dark. Cells were then washed with PBS and incubated with acini buffer (120 mM NaCl, 4 mM KCl, 1 mM $CaCl_2$, 1.2 mM KH_2PO_4, 1 mM $MgSO_4$, 15 mM HEPES, 0.1% BSA, 10 mM glucose, and pH 7.4) for 3 minutes at 37°C in the dark for de-esterification. Cells were then stimulated with 1 mM acetylcholine for 1.5 minutes while exciting at a wavelength of 488 nm using an Argon/2 laser. Emission was acquired at 520 nm using a BP 500-550 filter on a Zeiss LSM 510 confocal microscope. Images were acquired in a time series of 180 frames at 0.5-second intervals for 90 seconds at 40x magnification. To calculate the maximal intensity (F_{max}), incubation

with 10μM ionomicin in presence of 10mM $CaCl_2$ was performed. Ca^{2+} concentration was determined as described (*27*).

Cell death assay: SH-SY5Y cells were treated with gp120 (0.15 nM) overnight. Cell death was measured using the APO-BrdU TUNEL Assay Kit (Invitrogen Corporation, Carlsbad, CA) following the manufacturer's instructions with slight modifications. All centrifugations steps were done at 6000 rpm. In brief, all cells were detached, centrifuged for 6 minutes, fixed with 2% paraformaldehyde for 20 minutes and centrifuged for 6 minutes. Cells were then permeabilized with 70% ethanol for 24 hours at -20°C, centrifuged for 6 minutes, resuspended in wash buffer, and centrifuged again. Then, cells were incubated with labeling solution for 24 hours at room temperature, washed with 1 mL of rinse buffer, and centrifuged. This step was followed by incubation with antibody staining solution for 1 hour at room temperature. After this, cells were washed with PBS, mounted in glass slides, and visualized with an Axiovert 200M confocal microscope.

Real-time PCR: Total RNA was isolated from SH-SY5Y cells or mouse brains using the TRIzol reagent (Invitrogen Corporation, Carlsbad, CA). The cDNA synthesis was carried out using 1 μg of total RNA with the iScript™cDNA Synthesis Kit (Bio-Rad Laboratories, Inc., Hercules, CA) following the manufacturer's instructions. Real-time PCR experiments were done using the iQ™ SYBR® Green Supermix (Bio-Rad Laboratories, Inc., Hercules, CA) in a Mastercycler® ep realplex Thermal Cycler (Eppendorf, Hauppauge, NY). The following primer pairs were used: fwd = 5'-GCTCCGGGACTCAACATG-3' and rev = 5-GGGATTGTAGTTCTTGACCAGC-3' for CHRNA7, fwd = 5'-AGCACCTTCAACCCTCA-3' and rev = 5'-AGTCGAGTGGTTTGGCT-3' for EGR1 and fwd = 5'-GCTCTCTGCTCCTCCTGTTC-3' and rev = 5'-GACTCCGACCTTCACCTTCC-3' for GAPDH.

Animals: Transgenic mice expressing the HIV-1 coat protein gp120 under the regulatory control of a modified murine glial fibrillary acidic protein (GFAP) gene were obtained from a previously established line (Toggas et al., 1996) and housed in clear plastic cages, maintained in a temperature- and humidity-controlled room on a 12-hour light/dark cycle with food and water provided *ad libitum*. Animals from the background strain B6SJLF were used as control.

Western blot: Transgenic (tg) and wild type (WT) mice were sacrificed by cervical dislocation, brains were placed on ice and dissected to separate the striatum and hippocampus. Pulverized tissue was transferred to 15-mL tubes containing cold RIPA buffer (10mL/g) supplemented with a protease inhibitor cocktail. The sample was agitated for 30 seconds and incubated for 1 hour at 4°C, shaking. Then, the sample was centrifuged at 14,000 rpm for 15 minutes at 4°C and protein in the lysates was quantified with the Pierce BCA kit (Pierce Biotechnology, Rockford, IL). Samples containing 50 μg of total protein were loaded on a 4%-20% linear gradient polyacrylamide gel (Bio-Rad Laboratories, Hercules, CA), and electrophoresis was done at 100 mV for 1 hour at RT. Proteins were transferred to a PVDF membrane (Amersham Biosciences, Piscataway, NJ) at 100 mV for 1 hour. Non-specific binding was blocked with 5% non-fat dry milk in TBS-T (1X) for 1 hour at RT. The membrane was then incubated with a polyclonal rabbit anti-α7nAChR (1:1000, Millipore) diluted in 5% skim milk, overnight at 4°C, shaking. Three consecutive washes with TBS-T (5 minutes each) were done to eliminate excess antibody and the membrane was incubated with an anti-rabbit antibody conjugated to HRP (1:5000, Abcam) for 1 hour at room temperature. Antibody binding was detected with the ECL Plus Western Blotting detection system (Amersham Biosciences) and developed using Kodak BioMax MS film (Kodak, New Heaven, CT).

Cell culture and treatment with gp120, SDF-1α, or AMD3100: SH-SY5Y cells were grown in DMEM/F12 media supplemented with 10% FBS and 1% antibiotic/antimicotic solution (Sigma-Aldrich, St. Louis, MO) and treated for 24 hours. Several compounds were used at various concentrations: $gp120_{IIIB}$ (Fitzgerald Industries International, Inc., Concord, MA), SDF-1α (EMD Chemicals, Inc., Gibbstown, NJ) at 0.3 μg/mL; AMD3100 (EMD Chemicals, Inc., Gibbstown, NJ) at 1 μM, where pre-treatment was carried out 10 minutes before the addition of gp120 or SDF-1α; and α-bungarotoxin (Invitrogen Corporation, Carlsbad, CA) at 1 μM, where pre-treatment was carried out 10 minutes before the addition of gp120 or SDF-1α.

Results

gp120 increases α-bgtx binding and acetylcholine-stimulated currents in SH-SY5Y cells

To study the effects of gp120 on α7-nAChR expression, SH-SY5Y cells were treated with different concentrations of gp120. Alexa Fluor 488-α-bgtx was used to detect α7-nAChRs. As shown in Fig. 1A-B, cells treated with various concentrations of gp120 showed an increase in α-

bgtx binding, consistent with higher levels of α7-nAChRs. To determine if the increase in α-bungarotoxin binding correlates with an increase in functional nicotinic acetylcholine receptors, we measured currents in response to stimulation with 1 mM acetylcholine (ACh) using the whole-cell configuration of the patch clamp technique. As shown in Fig. 1C-D cells treated with different concentrations of gp120 presented an increase in whole-cell current density in response to ACh. These results show that gp120 treatment leads to an increase in functional α7-nAChRs.

gp120 effects are mediated by the CXCR4 receptor

It has been shown that gp120 activates the chemokine receptor CXCR4, which is expressed in SH-SY5Y cells (10). We hypothesized that this receptor was involved in the gp120-induced up-regulation of α7-nAChRs on the basis of findings by Luo *et al.* and Criado and del Toro, which showed that SDF-1α, the endogenous CXCR4 agonist, up-regulates Egr-1, a known transcription factor for the α7-nAChR. As shown in Fig. 2A, the CXCR4 antagonist, AMD3100, prevented the increase in α-bgtx binding observed after treatment with gp120. Pre-treatment with AMD3100 also prevented the gp120-induced increase in ACh-stimulated currents (Fig. 2B). These results reveal that CXCR4 activation by gp120 is necessary for the up-regulation of the α7-nAChR. On the basis of these findings, we proceeded to test if activation of the CXCR4 receptor by its endogenous ligand, SDF-1, would have similar effects on α-bungarotoxin binding and ACh-stimulated currents. Fig. 2B shows that SDF-1α treatment resulted in increased α-bungarotoxin binding and ACh-stimulated currents, similar to what was observed after gp120 treatment. The α7-nAChR up-regulation can be prevented by the MEK inhibitor PD98059, suggesting that the effect of SDF1 requires activation of the MAP kinase pathway (supplemental material, Fig. S2).

gp120 increases acetylcholine stimulated calcium movement

Of all the nicotinic receptors, the α7-nAChR has the highest permeability to Ca^{2+} ions (*28, 29*). Taking this fact into consideration, we decided to measure the intracellular Ca^{2+} concentration after stimulating SH-SY5Y cells with ACh. As shown in Fig. 3, control cells stimulated with ACh had an increase in intracellular Ca^{2+} concentration ($[Ca^{2+}]_i$) that peaked around 100 nM (supplemental material, VS1). This increase in $[Ca^{2+}]_i$ can be blocked by addition of MLA (supplemental material VS3), a selective antagonist for the α7-nAChR, suggesting its role in mediating this effect. In contrast, cells treated with gp120 (0.15 nM) had an increase in $[Ca^{2+}]_i$ that peaked at around 1,100 nM (supplemental material VS2), 11 times more than the $[Ca^{2+}]_i$ observed in control cells. Once more, this effect can be inhibited by addition of MLA (supplemental material VS4), confirming the involvement of the α7-nAChR in mediating the increase in $[Ca^{2+}]_i$.

gp120-induced up-regulation of α7-nAChRs leads to cell death

When considering the effects of the increase in α7-nAChRs for cellular function, it is important to keep in mind that large increases in intracellular Ca^{2+} have been shown to induce cell death (*30*). Moreover, treatment with gp120 has been shown to induce cell death in neuroblastoma cells (*10*). To test the hypothesis that α7-nAChR up-regulation plays a role in the gp120-induced cell death observed in SH-SY5Y cells, we performed TUNEL staining after treatment with gp120 with and without the addition of α-bgtx, an α7-nAChR antagonist. Fig. 4 shows that antagonizing α7-nAChRs with α-bgtx reduced the percentage of cells undergoing cell death after treatment with gp120. These data suggest that increased activity of α7-nAChRs contributes to gp120-induced cell death.

α7-nAChR and Egr1 mRNA levels are up-regulated in SH-SY5Y cells treated with gp120

The experiments performed in SH-SY5Y cells suggest that CXCR4 activation by either gp120 or SDF-1 results in increased levels of functional α7-nAChRs. The CXCR4 receptor has been shown to activate the early growth response protein, EGR1 (*23*). The immediate early gene, EGR1, binds to the promoter region of the α7 gene and increases transcription (*24, 31*). Real-time PCR on SH-SY5Y cells treated with gp120 for different periods of time showed a fast and transient up-regulation of EGR1 with a peak of 8.4-fold increase after 30 minutes. To test if α7-nAChRs mRNA levels are increased after treatment with gp120, real-time PCR was performed using CHRNA7-specific primers. Fig. 5 shows that EGR1's transient up-regulation was accompanied by an approximately 4-fold increase in α7 mRNA levels that peaked 60 minutes after gp120 treatment. Consistently, increased α7-nAChR currents were observed as early as 1 hour after gp120 treatment and persisted for at least 48 hours (supplemental material, Fig. S1).

α7-nAChR mRNA and protein levels are increased in gp120 transgenic mice

Quantitative RT-PCR and Western blot experiments showed that mRNA and protein levels of α7-nAChRs are increased in the CNS of gp120-transgenic mice (Fig. 5). However, the up-regulation of α7-nAChRs was observed in the striatum, a region affected in HAND patients, but not in the hippocampus (supplemental material, Fig. S3). Interestingly, the striatum expresses high levels of the CXCR4 receptor and, furthermore, the expression of this receptor is increased in HIV+ patients (*32*). These findings are in aggreement with our data from SH-SY5Y cells and previous studies that implicate the CXCR4 in gp120-induced neurotoxicity (*33, 34*).

Discussion

We have developed a model for gp120 neurotoxicity, in which activation of the CXCR4 receptor by gp120 or SDF1 leads to activation of the MAPK pathway, increased EGR1 levels, and up-regulation of α7-nAChRs that triggers cell death (Fig. 6). This model is supported by data showing that treatment of SH-SY5Y cells with gp120 results in higher expression of α7-nAChRs, which are highly permeable to Ca^{2+}. Increased intracellular Ca^{2+} can lead to cell death and has been associated with neuronal death in neurodegenerative diseases (*35*). Along these lines, over-expression of α7-nAChRs has been shown to play a role in neurological disorders (*36*). Studies have shown that in neuronal cultures, gp120 can induce an increase in Ca^{2+} levels, leading to neuronal injury, an effect that can be blocked with memantine (*37*). Interestingly, besides being an antagonist for the NMDA receptor, memantine has been shown to also act as an antagonist of α7-nAChRs (*38*). Moreover, subsequent studies have shown involvement of CXCR4 in the neurotoxic effects of gp120 (38). These results suggest that other proteins, besides the NMDA receptor, contribute to gp120 neurotoxicity.

TUNEL staining showed that exposure to gp120 increases cell death in SH-SY5Y cells, consistent with previous studies (*37, 39*). Our experiments show that pre-treatment with α-bgtx reduced the percentage of cells undergoing cell death after gp120 treatment. These data suggest that the gp120-induced up-regulation of functional α7-nAChRs may be detrimental to neurons and implicates the α7-nAChR as a potential key player in HIV pathogenesis. It is important to mention that desensitization of α7-nAChRs by chronic exposure to different agonists, such as nicotine, has been associated to receptor up-regulation and neuroprotection (*40, 41*). This scenario differs from the gp120-induced α7-nAChR up-regulation and toxicity in that the observed gp120 effects involve activation of the CXCR4 receptor. It is conceivable that chronic nicotine exposure leads to an increase in α7-nAChRs to compensate for the reduced receptor activity due to desensitization. In contrast, our data suggest that gp120 activates CXCR4 receptors leading to an increase in functional α7-nAChRs without involving desensitization. Whereas small influxes in Ca^{2+} associated with tonic small levels of activation of α7-nAChRs might be neuroprotective, large influxes of Ca^{2+} as consequence of receptor up-regulation appear to be citotoxic (*42, 43*).

Many studies have shown that gp120 binding to the CXCR4 or CCR5 receptors elicits intracellular responses that include the activation of the MAPK pathway, transcription factors, and ion channels (*32, 44-46*). In the course of HIV infection, the virus exhibits changes in its tropism: from an R5 variant to an X4 variant (*15*). By the time HIV-1 becomes capable of infecting cells through the use of the CXCR4, there is an associated CD4 cell decline and disease progression (*20*). This rapid decrease in CD4 cell count associated with CXCR4 tropism, couples with an increased risk of developing HAND (*18*). This correlates with the fact that hippocampal and basal ganglia neurons express CXCR4 but not CCR5, which is present in glial cells (*32*). Previous studies have demonstrated that activation of CCR5 can lead to cell death in the presence of gp120 *(51)*, however, our experiments show that $gp120_{IIIB}$ as well as SDF-1α, both specific to CXCR4, induce an up-regulation of the α7-nAChR. Moreover, this effect is abolished by pre-treatment with the CXCR4 antagonist AMD3100, ruling out the contribution of CCR5 in our experimental setting. These results show that CXCR4 activation is necessary for the up-regulation of α7-nAChRs, and CXCR4-expressing neurons would be more susceptible to the effects of HIV infection.

CXCR4 activates the MAPK pathway and its activation by SDF-1α induces the up-regulation of Egr-1, a transcription factor capable of stimulating the expression of the α7 gene (CHRNA7) (*23, 24*). Our experiments show that treating SH-SY5Y cells with SDF-1α induced a functional up-regulation of α7-nAChRs, as seen by increased α-bungarotoxin binding and larger

ACh-stimulated whole-cell currents. Furthermore, qRT-PCR experiments showed that gp120 and SDF-1α treatment of SH-SY5Y cells induced a rapid and transient increase in Egr-1 mRNA expression levels concomitant with an increase in α7-nAChRs mRNA expression levels. Together, these results provide a molecular mechanism as to how the α7-nAChR could be up-regulated in neurons in the context of an HIV-infected CNS.

In HAND, the sustained immune response can produce neuronal injury despite viral control (*47*). In the brain, viral particles such as gp120, can cause macrophages and/or astrocytes to release various cytokines and chemokines (nitric oxide, TNF-α, IL-1, IL-6, MCP-1) resulting in further neuronal stress and cell death. Production of IL-1 by astrocytes leads to an increase in SDF-1 (*25*). The α7-nAChR has been shown to contribute to the regulation of inflammation in macrophages (the cholinergic anti-inflammatory pathway); however, the sustained immune response and increased production of SDF-1 could cause alterations in α7-nAChR function. Immune responses depend on the equilibrium between pro- and anti-inflammatory cytokines and alterations of this equilibrium could convert a beneficial inflammatory response into a pathologic process (*48*). In this context, gp120 and SDF1 could have synergistic effects, leading to up-regulation of the α7-nAChR and subsequent neuronal death. Interestingly, a similar up-regulation of α7-nAChR has been observed in macrophages derived from HIV+ donors (our unpublished data), but the implications of these findings for macrophage function and inflammation remain to be explored.

To further validate our results in an *in-vivo* model, we used transgenic mice that express HIV-gp120 under the GFAP promoter. HIV-gp120 has been shown to induce neuropathological changes in mice similar to those seen in HAND patients (*49, 50*), making it a suitable model to study gp120-mediated neurotoxicity. Consistent with the results from *in-vitro* experiments, we observed that α7-nAChRs mRNA and protein levels are increased in the CNS of gp120 transgenic mice. However, the α7-nAChRs up-regulation appears to be restricted to the striatum, a component of the basal ganglia and a region greatly affected in HAND patients (*47*).

Our results are in agreement with experiments performed by Kaul, M., et al. 2007 (*51*) showing that $gp120_{IIIB}$ and SDF1 are neurotoxic only in the presence of the CXCR4 receptor. In these experiments it was shown that inhibiting p38 prevented the gp120 and SDF1 neurotoxicity. Interestingly, it has been shown that induction of EGR1 requires p38 activity (*52*). These data, in conjunction with our results, suggests the existence of a neurotoxic pathway in which CXCR4 activation leads to a p38 dependent EGR1 induction that increases α7-nAChRs expression levels and causes cell death.

In conclusion, our experiments suggest that the α7-nAChR is a previously unrecognized contributor to HIV neurotoxicity. Drugs that antagonize the CXCR4 or α7-nAChR receptors might be of therapeutic benefit in the treatment of HAND.

Acknowledgments

This research was supported by NIH Grant SNRP-U54N54301. Coral Capó-Vélez was supported by the RISE-MBRS-NIH program (2R25GM061151). Wilfredo García-Beltran was supported by the Minority Access to Research Careers (MARC)-MBRS-NIH program.

References:

1. UNAIDS/WHO 2008 report on the global AIDS epidemic.
2. V. Tozzi *et al.*, *J Acquir Immune Defic Syndr* **45**, 174 (Jun 1, 2007).
3. N. Sacktor *et al.*, *Neurology* **56**, 257 (Jan 23, 2001).
4. A. K. Njamnshi *et al.*, *J Neurol Sci* **285**, 149 (Oct 15, 2009).
5. N. Sacktor, *J Neurovirol* **8 Suppl 2**, 115 (Dec, 2002).
6. M. H. Wong *et al.*, *Neurology* **68**, 350 (Jan 30, 2007).
7. M. Kaul, *Curr Opin Neurol* **22**, 315 (Jun 1, 2009).
8. M. Ghafouri, S. Amini, K. Khalili, B. E. Sawaya, *Retrovirology* **3**, 28 (2006).
9. M. P. Mattson, N. J. Haughey, A. Nath, *Cell Death Differ* **12 Suppl 1**, 893 (Aug, 2005).
10. G. Bardi, R. Sengupta, M. Z. Khan, J. P. Patel, O. Meucci, *J Neurovirol* **12**, 211 (Jan 1, 2006).
11. E. B. Dreyer, P. K. Kaiser, J. T. Offermann, S. A. Lipton, *Science* **248**, 364 (Apr 20, 1990).
12. S. Okamoto *et al.*, *Cell Stem Cell* **1**, 230 (Aug 16, 2007).
13. J. Buzy *et al.*, *Brain Res* **598**, 10 (Dec 11, 1992).
14. L. Bracci, L. Lozzi, M. Rustici, P. Neri, *FEBS Lett* **311**, 115 (Oct 19, 1992).
15. E. A. Berger, P. M. Murphy, J. M. Farber, *Annu Rev Immunol* **17**, 657 (Jan 1, 1999).
16. C. Lee *et al.*, *J Leukoc Biol* **74**, 676 (Nov, 2003).
17. C. Conejero-Goldberg, P. Davies, L. Ulloa, *Neurosci Biobehav Rev* **32**, 693 (2008).
18. B. Giunta *et al.*, *Brain Res Bull* **64**, 165 (Aug 30, 2004).
19. R. B. Rock *et al.*, *J Neuroimmune Pharmacol* **3**, 143 (Sep, 2008).
20. E. H. Stalmeijer *et al.*, *J Virol* **78**, 2722 (Mar, 2004).
21. D. M. T. Nieves, M. Plaud, V. Wojna, R. Skolasky, L. M. Meléndez, *J Neurovirol* **13**, 315 (Aug 1, 2007).
22. D. Misse *et al.*, *Blood* **93**, 2454 (Apr 15, 1999).
23. Y. Luo, J. Lathia, M. Mughal, M. P. Mattson, *J Biol Chem* **283**, 24789 (Sep 5, 2008).
24. M. Criado *et al.*, *J Neurosci* **17**, 6554 (Sep 1, 1997).
25. H. Peng *et al.*, *Glia* **54**, 619 (Nov 1, 2006).
26. H. Geminder *et al.*, *J Immunol* **167**, 4747 (Oct 15, 2001).
27. M. F. Navedo, G. C. Amberg, M. Nieves, J. D. Molkentin, L. F. Santana, *J Gen Physiol* **127**, 611 (Jun 1, 2006).
28. D. S. McGehee, L. W. Role, *Annu Rev Physiol* **57**, 521 (1995).
29. P. Seguela, J. Wadiche, K. Dineley-Miller, J. A. Dani, J. W. Patrick, *J Neurosci* **13**, 596 (Feb, 1993).
30. M. P. Mattson, S. L. Chan, *Nat Cell Biol* **5**, 1041 (Dec 1, 2003).
31. U. Nagavarapu, S. Danthi, R. T. Boyd, *J Biol Chem* **276**, 16749 (May 18, 2001).
32. P. van der Meer, A. M. Ulrich, F. Gonzalez-Scarano, E. Lavi, *Exp Mol Pathol* **69**, 192 (Dec, 2000).
33. J. Zheng *et al.*, *J Neuroimmunol* **98**, 185 (Aug 3, 1999).
34. J. Hesselgesser *et al.*, *Curr Biol* **8**, 595 (May 7, 1998).
35. P. Marambaud, U. Dreses-Werringloer, V. Vingtdeux, *Mol Neurodegener* **4**, 20 (2009).
36. S. E. Counts *et al.*, *Arch Neurol* **64**, 1771 (Dec, 2007).
37. S. A. Lipton, *Neurology* **42**, 1403 (Jul, 1992).
38. Y. Aracava, E. F. Pereira, A. Maelicke, E. X. Albuquerque, *J Pharmacol Exp Ther* **312**, 1195 (Mar, 2005).
39. M. V. Catani *et al.*, *J Neurochem* **74**, 2373 (Jun, 2000).
40. R. R. Jonnala, J. J. Buccafusco, *J Neurosci Res* **66**, 565 (Nov 15, 2001).
41. M. J. De Rosa, C. Esandi Mdel, A. Garelli, D. Rayes, C. Bouzat, *J Neuroimmunol* **160**, 154 (Mar, 2005).
42. E. M. Johnson, Jr., T. Koike, J. Franklin, *Exp Neurol* **115**, 163 (Jan, 1992).
43. V. V. Uteshev, E. M. Meyer, R. L. Papke, *Brain Res* **948**, 33 (Sep 6, 2002).
44. Q. H. Liu *et al.*, *Proc Natl Acad Sci U S A* **97**, 4832 (Apr 25, 2000).
45. T. S. Stantchev, C. C. Broder, *Cytokine Growth Factor Rev* **12**, 219 (Jun-Sep, 2001).
46. M. Del Corno *et al.*, *Blood* **98**, 2909 (Nov 15, 2001).
47. S. P. Woods, D. J. Moore, E. Weber, I. Grant, *Neuropsychol Rev* **19**, 152 (Jun, 2009).
48. E. Tyagi, R. Agrawal, C. Nath, R. Shukla, *Innate Immun* **16**, 3 (Feb).
49. S. M. Toggas *et al.*, *Nature* **367**, 188 (Jan 13, 1994).
50. R. D'Hooge, F. Franck, L. Mucke, P. P. De Deyn, *Eur J Neurosci* **11**, 4398 (Dec, 1999).
51. M. Kaul, Q. Ma, K.E. Medders, M.K. Desai, S.A. Lipton, *Cell death and diff* **14**, *296* (2007).

52. S. Kenzel, S. Santos-Sierra, S.D. Deshmukh, I. Moller, B. Ergin, K.A. Fitzgerald, E. Lien, s. Akira, D.T. Golenbock, P. Henneke, Infect Immun **77**, 2474 (2009)

Figure Legends:

Figure 1. Increased α-bungarotxin binding and ACh-stimulated currents in SH-SY5Y cells after treatment with gp120. (A) Alexa Fluor 488-conjugated α-bungarotoxin binding to SH-SY5Y cells treated with 0.15, 15, 150, or 1500 nM gp120, or control cells. (B) The normalized fluorescence intensity for control SH-SY5Y cells was 100.0 ± 6.0% (*n* = 16). Cells treated with 0.15, 15, 150, and 1500 nM showed a percent fluorescence intensity of 163.5 ± 26.7% (*n* = 12), 174.6 ± 10.7% (*n* = 13), 150.4 ± 9.1% (*n* = 12), and 167.5 ± 26.3% (*n* = 17), respectively. (C) Whole-cell representative current traces recorded from control SH-SY5Y cells or cells treated with 0.15, 15, 150 and 1500nM gp120. Currents were recorded in response to application of a 1mM acetylcholine pulse at a holding potential of -100mV. (D) The average density for acetylcholine-stimulated currents recorded from control SH-SY5Y cells was 18.9 ± 3.9 pA/pF (*n* = 15). For cells treated with 0.15, 15, 150 and 1500nM gp120, the average current density was 32.1 ± 13.1 pA/pF (*n* = 4), 48.5 ± 8.1 pA/pF (*n* = 7), 41.7 ± 16.9 pA/pF (*n* = 7) and 44.7 ± 9.5 pA/pF (*n* = 12) respectively. * = p-value < 0.05

Figure 2. The CXCR4 receptor mediates the gp120-induced up-regulation of the α7-nAchR. (A) Alexa-488-conjugated-α-bungarotoxin binding to control SH-SY5Y cells or cells treated with 1500 nM gp120, 1500 nM gp120 plus AMD3100 (0.1μM), SDF1 (0.3 μg/ml), or SDF1 (0.3 μg/ml) plus AMD3100 (0.1 μM). (B) The percent fluorescence intensity for control SH-SY5Y cells was 100.0 ± 6.5% (*n* = 14). Cells treated with 1500nM gp120 showed a percent fluorescence intensity of 153.9 ± 13.1% (*n* = 12). The percent fluorescence for cells treated with 1500nM gp120 plus AMD3100 was 90.2 ± 9.7% (*n* = 15). Cells treated with SDF1 had a percent fluorescence intensity of 207.1 ± 17.3% (*n* = 11). (C) Representative whole-cell current traces of control SH-SY5Y cells, cells treated with 1500 nM gp120, gp120 plus AMD3100, SDF1, or SDF1 plus AMD3100. (D) The average current density for control cells was 18.9 ± 3.9 pA/pF (*n* = 15). Cells treated with gp120, gp120 plus AMD3100, SDF1, and SDF1 plus AMD3100 showed an average current density of 44.7 ± 9.4 pA/pF (*n* = 12), 20.7 ± 5.9 pA/pF (*n* = 9), 58.9 ± 13.1 pA/pF (*n* = 5), and 16.0 ± 4.1 (*n* = 4), respectively. Currents were recorded as described for figure 1. * = p-value < 0.05

Figure 3. Increased Ca^{2+} mobilization after gp120 treatment. (A) gp120 exposure that induced up-regulation of the α7-nAChR led to a remarkable Ca^{2+} mobilization in SH-SY5Y cells. Our data using confocal microscopy suggest that neuroblastoma cells exposed to gp120 (0.15 nM) reach a higher intracellular calcium concentration ($[Ca^{2+}]_{in}$) (1,179 ± 222.0 nM) in response to ACh than do control cells (108.6 ± 9.2 nM). The Ca^{2+} mobilization can be blocked by pre-incubation with MLA, an antagonist of the α7-nAChR in gp120-treated (167.0 ± 48.0 nM) and control (51.7 ± 3.3 nM) cells.

Figure 4. α-bungarotxin treatment reduces gp120-induced cell death in SH-SY5Y cells. (A) TUNEL staining of control SH-SY5Y cells (left), cells treated with 0.15 nM gp120 (middle), or cells treated with 1.5 nM gp120 after incubation with 1 μM α-bungarotoxin (right). (B) The percent cell death in control cells (black) was 7.4 ± 1.8% (*n* = 6); in gp120 treated cells, 20.4 ± 5.4% (*n* = 4); and in cells treated with α-bgtx and gp120, 13.8 ± 3.3% (*n* = 2). * = p-value = 0.02

Figure 5. **Real-time PCR and Western blot analysis of α7-nAChR on SH-SY5Y and gp120-transgenic mice.** (A) SH-SY5Y cells treated with gp120 at different time points. Up-regulation of α7-nAChR is observed after exposure to gp120 (n = 3). (B) Levels of EGR1 mRNA increased transiently in SH-SY5Y cells after gp120 treatment (n=3). (C) An increase in the levels of α7-nAChR mRNA was observed in the striatum of gp120 transgenic mice (7.55 ± 0.77, *n = 3*) as compared with WT (1.0 ± 0.1, *n = 4*) animals. (D) Western blot analysis of protein extracts from striatum revealed an increase in α7-nAChR protein in gp120 transgenic mice as compared with WT.

Figure 6. Proposed mechanism for gp120-induced up-regulation of the α7-nAChR. Activation of CXCR4 by SDF-1 or gp120 causes activation of the Ras-Raf-MEK pathway. This leads to activation of Egr-1, a known transcription factor for the α7-nAChR gene (CHRNA7). Activation of Egr-1 leads to an increase in α7-nAChR mRNA levels.

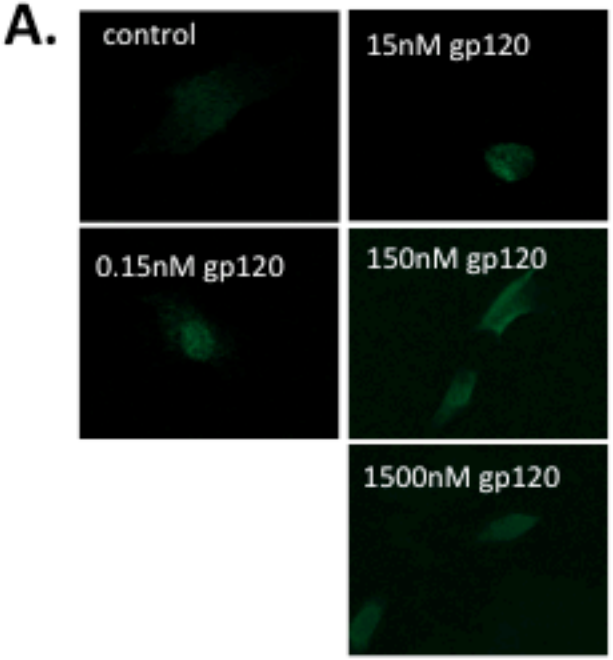

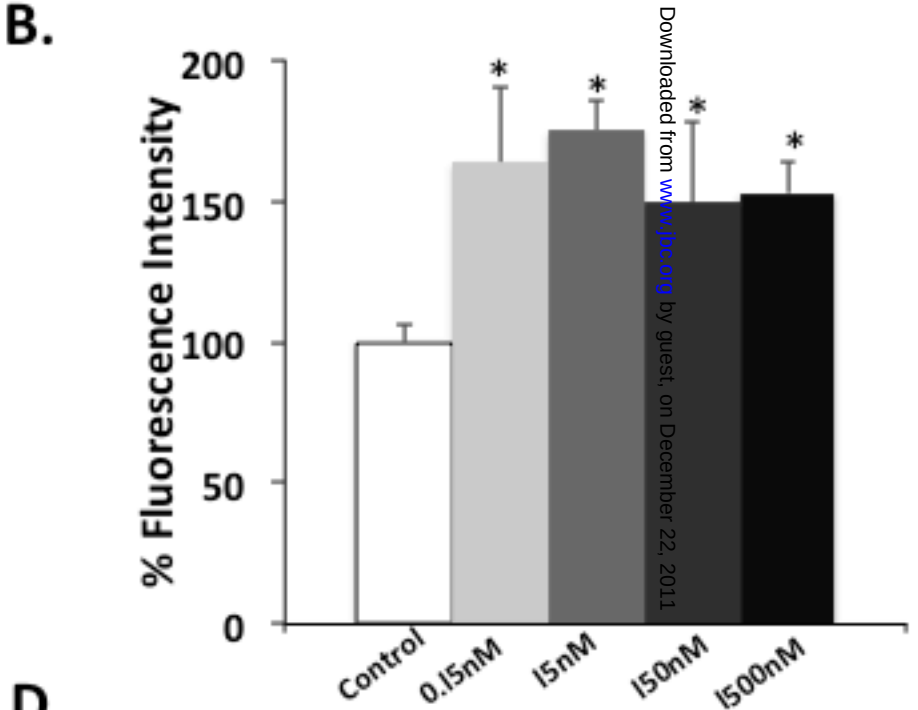

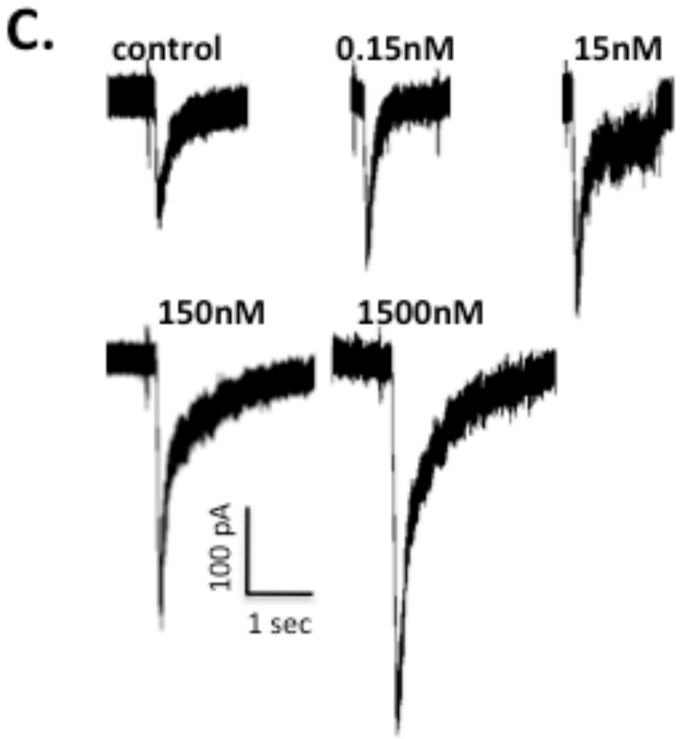

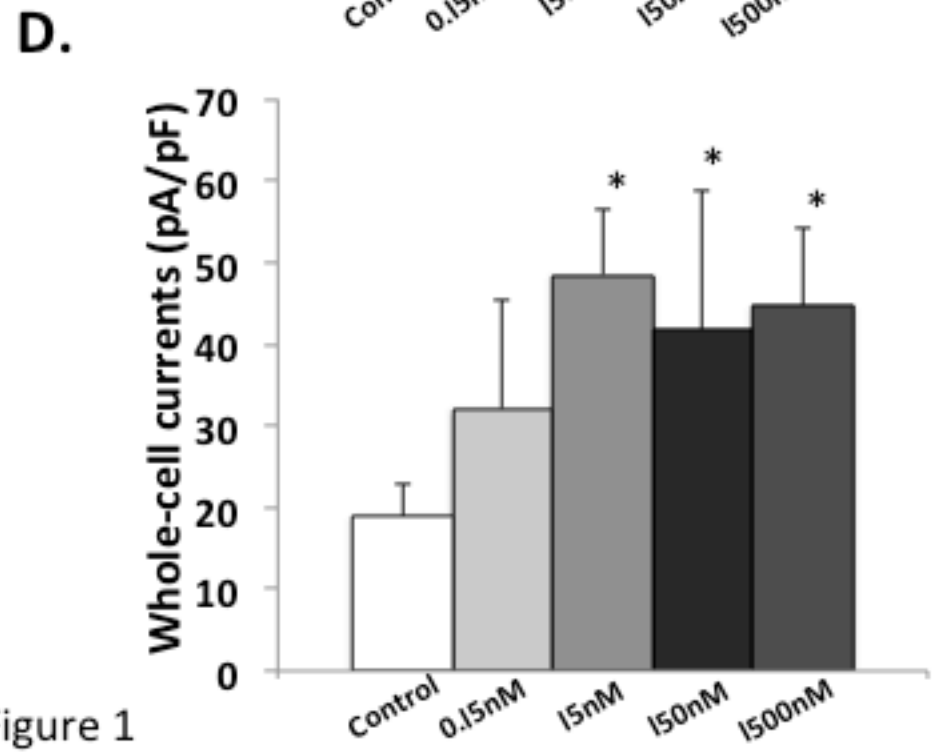

Figure 1

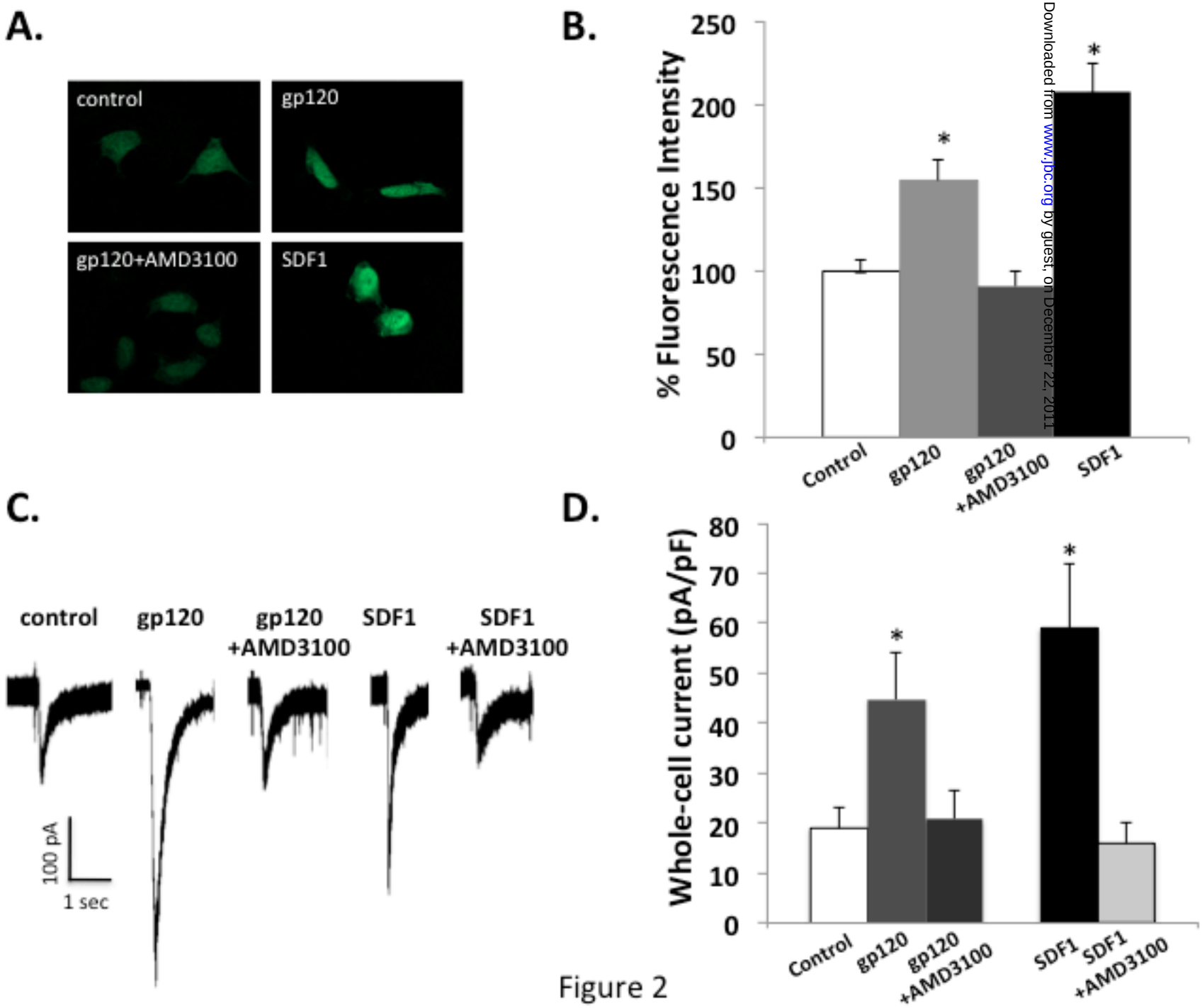

Figure 2

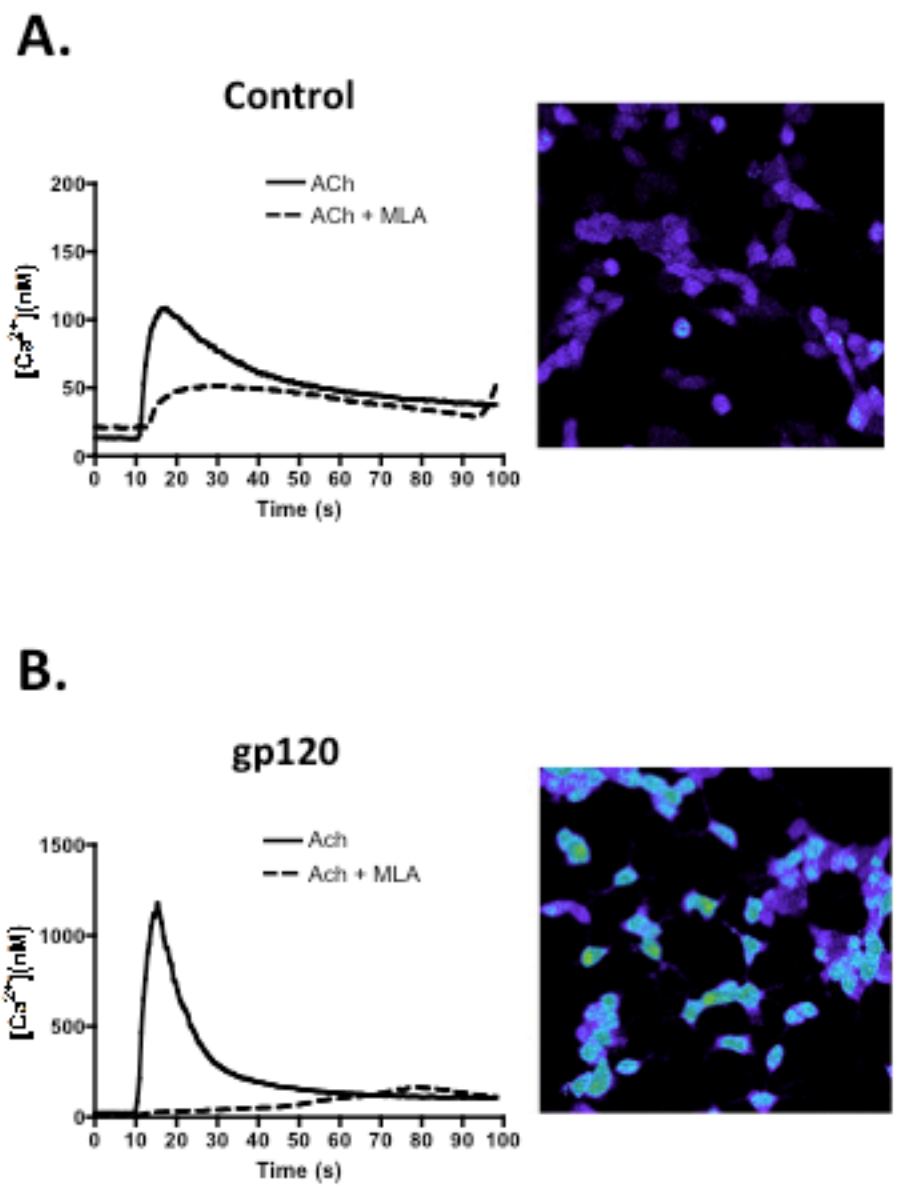

Figure 3

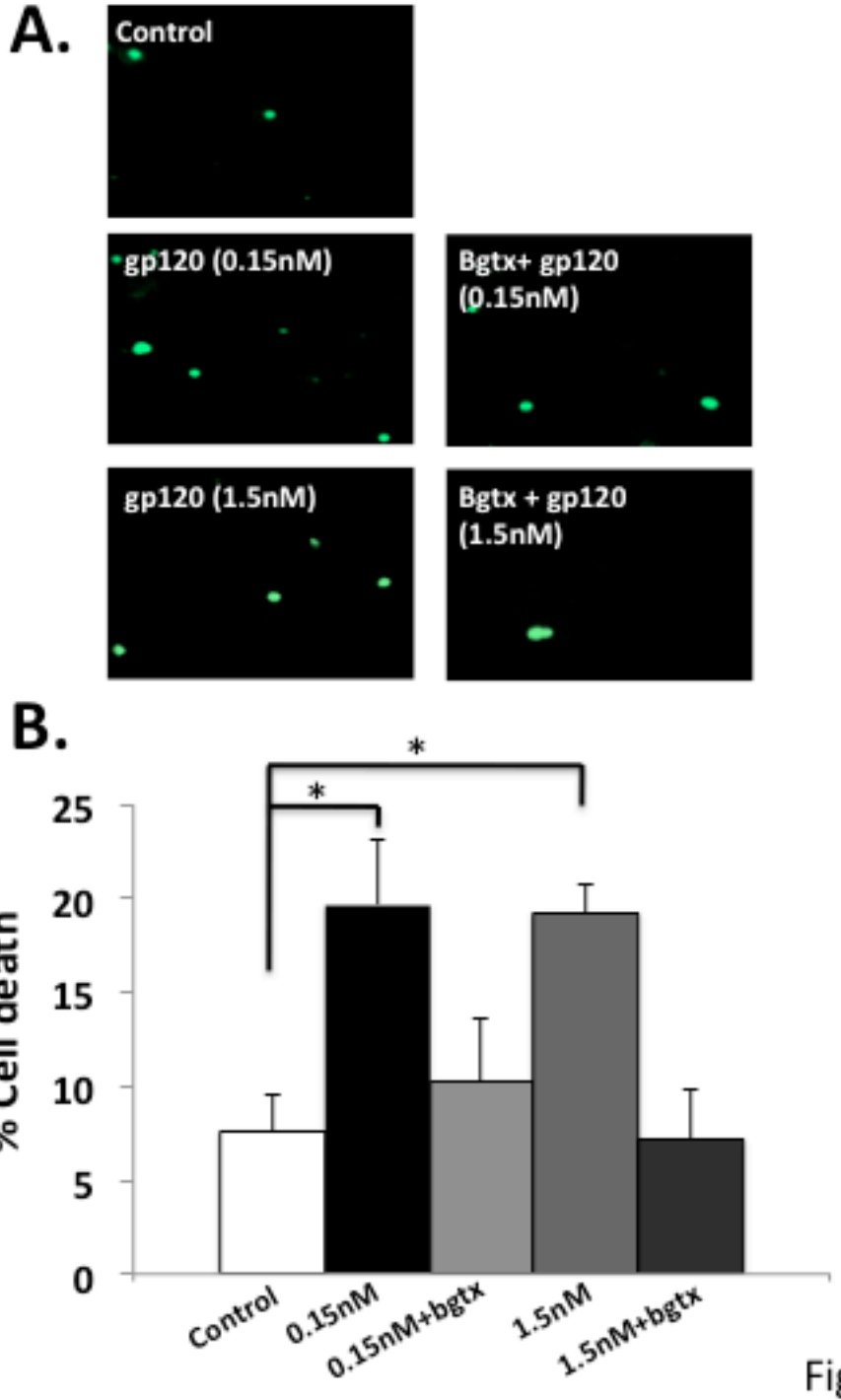

Figure 4

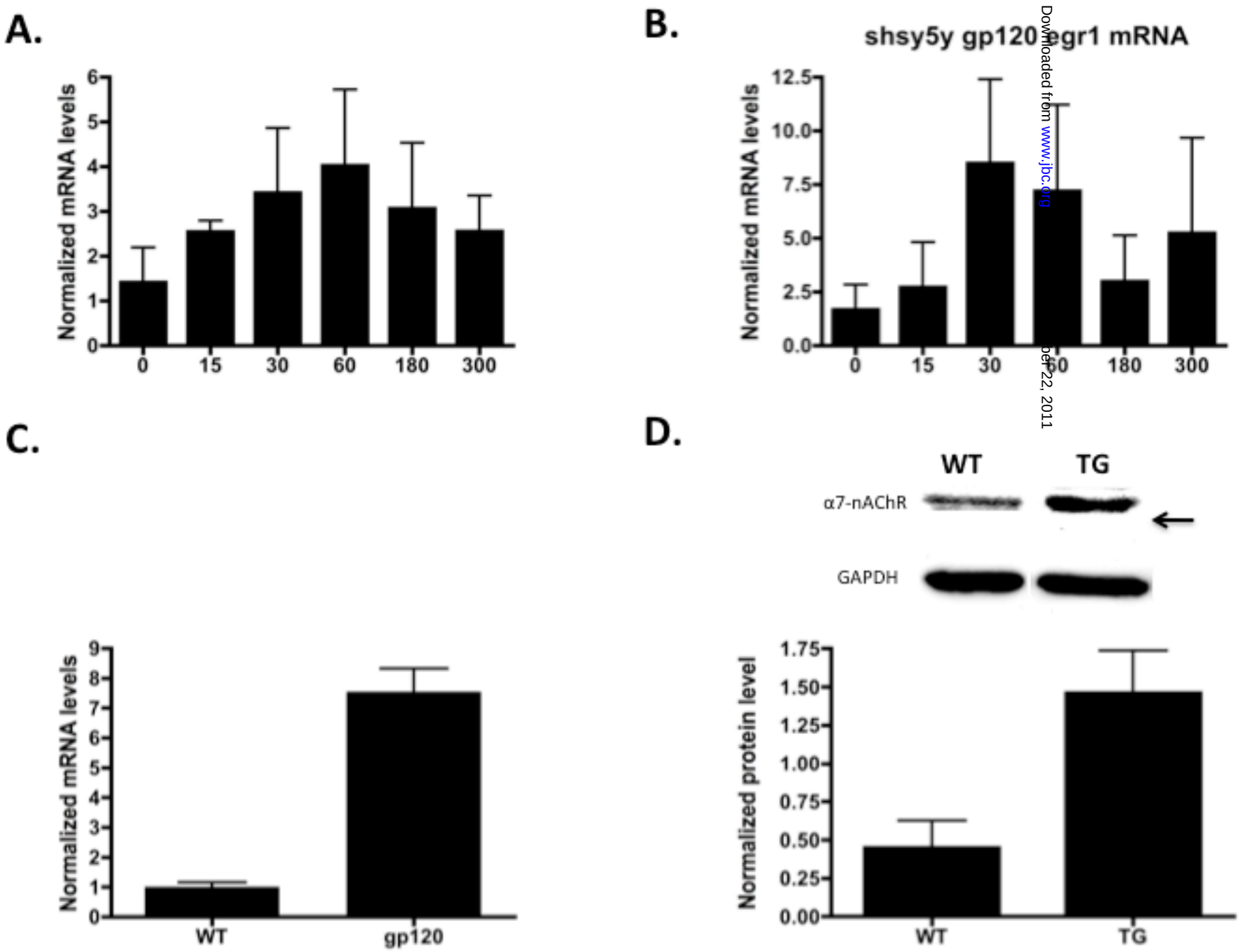

Figure 5

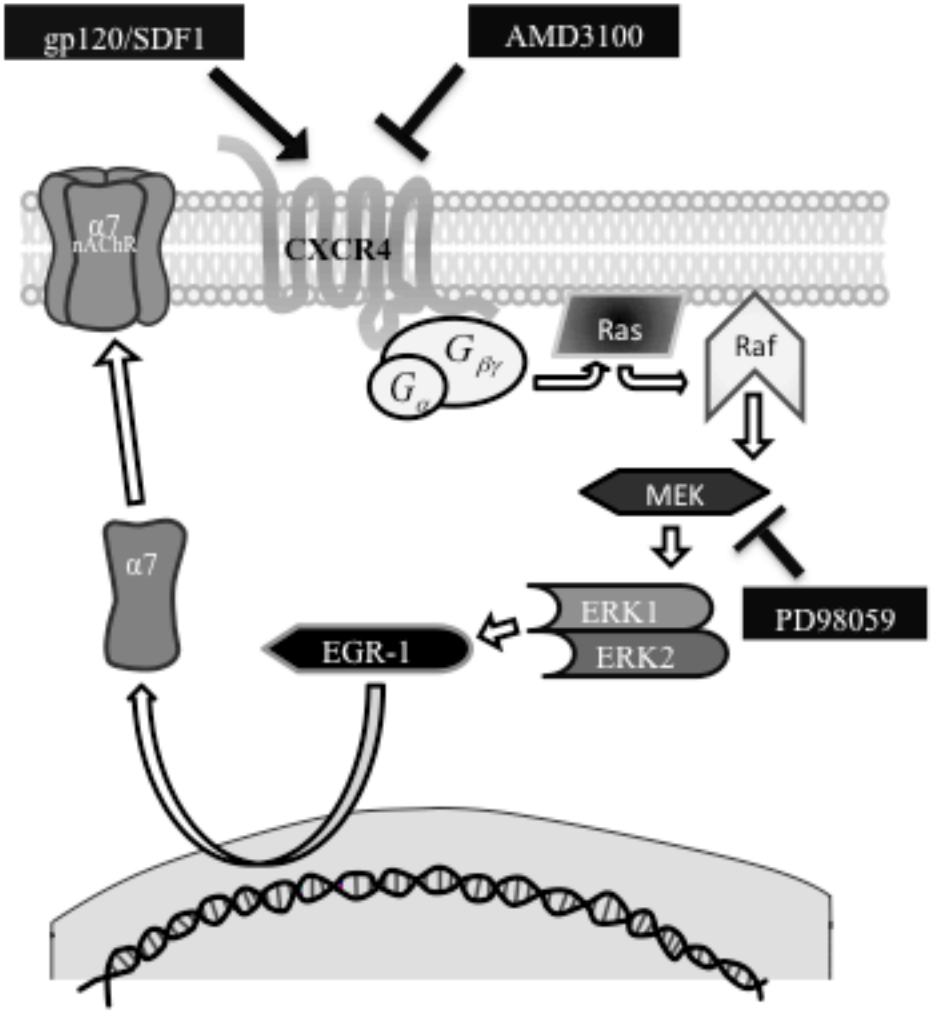

Figure 6